STALL EFFECTS AND BLADE TORSION - AN EVALUATION OF PREDICTIVE TOOLS

D. Petot[1], G. Arnaud[2], R. Harrison[3], J. Stevens[4], D. Teves[5], B.G van der Wall[6], C. Young[7] and E. Széchényi[1]

[1] ONERA, Chatillon, France
[2] Eurocopter, Marignane, France
[3] GKN Westland Helicopters, Yeovil, United Kingdom
[4] NLR, Amsterdam, Netherlands
[5] Eurocopter Deutschland, Ottobrunn, Germany
[6] DLR, Braunschweig, Germany
[7] DERA, Farnborough, United Kingdom

Abstract

Retreating side helicopter blades often experience stall when flying at high speeds or at high thrusts. There are a number of consequences to stall which result in significant increases in blade stresses, vibration levels, pitch link loads and required shaft power.
The prediction of these effects is at present still unsatisfactory. The models used in existing aeroelastic codes often lack accurate details of stall phenomena and rarely account for the effects of rotation on stall.
This paper presents some of the results and conclusions of a GARTEUR action group concerning stall effects and blade torsion. Seven different prediction models are described and tested against detailed measurements on a model rotor in a wind tunnel.
In order to identify the physical phenomena needing most attention in future developments, a series of calculations is carried out for a flight condition with a high load factor. These predictions use a range of hypotheses and models.
In this procedure the unsteady stall models used are evaluated with respect to experimental 2D hysteresis loops.
Conclusions are drawn relative to the state-of-the-art of dynamic stall models and of rotor calculations in general.

Introduction

Retreating side helicopter blades often experience stall when flying at high speed or at high thrusts. Though manufacturers strive to design stall free rotors for normal cruise conditions, it is impossible to avoid stall over the entire flight envelope of a helicopter and in particular at high load factors. There are a number of consequences to stall which result in:

- a significant increase in the shaft power required
- a significant increase in pitch link loads
- high blade root stress levels
- increased vibration levels

The prediction of these effects is at present still unsatisfactory. The models used in existing aeroelastic codes lack accurate details of stall phenomena and in particular take no account of the effect of rotation.

It is becoming increasingly clear that in all predictions it is necessary to consider real blades with their softness, particularly in torsion. Helicopter blades in flight experience notable blade deformations. These are becoming increasingly significant with the advent of new softer composite rotor designs and they need to be predicted correctly if rotor performances are to be determined accurately.

The prediction of blade torsional deformations is largely dependent on the ability to accurately predict unsteady aerodynamic moments in or out of stall.

At the present time, the confidence in predictive calculations is still generally poor.

In an attempt to establish the status on this subject and to clarify needs, a GARTEUR action group was set up with the following seven partners: DLR and ECD from Germany, DERA and WHL from the United Kingdom, ONERA and EC from France and NLR from the Netherlands.

The procedure adopted in the work of this action group was to:

- chose common aerofoil and rotor test data
- tune dynamic stall models for the chosen aerofoil
- compare experimental and predicted hysteresis loops of lift and pitching moment
- compare experimental and predicted rotor loads for varying complexities of the models
- compare results of the different partners and draw conclusions on the state of the art and on the need for further developments.

Rotor and aerofoil data

The rotor data chosen were obtained by ONERA in the S1MA wind tunnel on a 4.2 m diameter four bladed rotor. The blades had parabolic tips and were extensively instrumented with pressure transducers so that pressure integration yielded instantaneous lift and moment at five spanwise sections.
In order to study the stall phenomena the most heavily loaded flight condition ($C_T/\sigma = 0.125$) was chosen at an advance ratio of 0.4. This high lift value could only be obtained by a reduction of about 10% of the nominal speed of rotation of the rotor. Unfortunately blade torsion measurements were not available for this test case so that this parameter was also studied for a less loaded test case ($C_T/\sigma = 0.112$).
The rotor blades were made up of two aerofoils: OA213 from the root to 75% of span and OA209 from 90% of span to the tip. Between these two limits the aerofoil was interpolated linearly.

Two sets of relevant aerofoil data were available:

- Steady 2D aerodynamic coefficients for both OA209 and OA213 aerofoils obtained through very fine steady pressure measurements over a wide range of angle of attack and Mach number.
- Steady and unsteady 2D aerodynamic coefficients for the OA213 aerofoil at a Mach number of 0.18. The unsteady measurements were carried out with large angle of attack fluctuations (±10°) at various mean angle of attacks and three different reduced frequencies. The data was obtained for both normal and 22° swept flow.

The OA 213 aerofoil was chosen for the work on the dynamic stall models. The fact that the two sets of data were obtained

from two totally different experiments carried out in different wind tunnels with different instrumentation and different tunnel corrections leads to some inconsistencies which are reflected in the comparative analyses of the stall models.

Models and codes

Dynamic Stall models

DLR The aerofoil aerodynamic force coefficients normal and tangential to the chord line and the moment coefficient about the quarter chord point are represented by analytical functions [1]. All coefficients are the sum of separate analytic functions describing the fully separated flow conditions, the Kirchhoff flow, and the fully attached flow in terms of Mach number components, plus the non-circulatory parts due to accelerations. The attached flow coefficients are the sum of circulatory functions at positive and negative angles of attack, and a component due to an additional circulation resulting from a bubble at small Mach numbers. The characteristic parameters of these functions are the steady stall angle of attack at positive and negative angles. Additionally, the secondary vortex shedding leads to dynamic coefficients depending basically on the Strouhal number in frequency but is subject to random fluctuations in both frequency and magnitude. A yaw angle shifts the steady stall to larger angles.
When dynamic motion is applied to any or all flow components, the characteristic parameters such as the angle of attack and the stall angle become dynamic parameters, each represented by a separate transfer function. It is then possible to compute the attached flow hysteresis, the dynamic stall loops and very large lift coefficients under varying Mach number conditions [2].

DERA The dynamic stall model used for the DERA calculations is the first generation model developed by WHL (see below).

ECD uses CAMRAD/JA [3]. In this code different dynamic stall models are available. These stall models are based on a procedure using steady 2D aerofoil data in conjunction with dynamic delayed angles of attack. This approach allows the modelling of hysteresis effects for lift, moment and drag.
The corresponding procedure is characterised by requiring only a few additional parameters which allow a physical interpretation of their meaning. The implementation of the stall models is focused on solution robustness, easy handling and on large time steps which are typical for a frequency domain solver as used in CAMRAD/JA. In conjunction with the small number of parameters these restrictions limit the degree of sophistication of the stall models.
There are two basic approaches [4,5] to modify the section angle of attack derived from experimental data for determining the dynamic stall angles of attack. In the present case the angle of attack is delayed by the square root of the normalised angle of attack multiplied by a time delay coefficient. Different values of this time delay are used for lift, drag and moment according to the fit with the experimental data. The delayed angles of attack for lift, drag and moment are used as inputs for the 2D data table of the static coefficients. The lift coefficient is increased by the ratio of angle of attack and dynamic angle of attack in order to model the lift overshoot.

EC The dynamic stall model used by EC is derived from the ONERA-Edlin model [6]. However, an improvement has been made to this by substituting a specific Cm sub-model to the original differential equations. Indeed, the linear character of the equations is unable to reflect the sharp drop in pitching moment when stall occurs. The new sub-model is based on the idea that the increment of lift due to the unsteadiness depends on a powerful vortex convecting from the leading edge to the trailing edge and into the wake system. The displacement of this part of lift over the upper surface is modelled by the displacement of the aerodynamic centre over the aerofoil, thus creating extra pitching moment.

NLR uses the semi-empirical dynamic stall model proposed by Leishman and Beddoes [7] which is based on available analytical solutions for inviscid attached unsteady flow. This model was chosen because the published correlation between prediction and experiment is good, the model contains formulations for lift, drag and pitching moment, and it is based on physical phenomena. The model is two dimensional but typical 3D effects have been added when implemented in the comprehensive rotor code.
The unsteady aerofoil response is calculated by using the Duhamel integral in which the Wagner response function is used for a step change in angle of attack. The model makes use of the Kirchhoff formulation for the description of an aerofoil polar, in which the lift, drag and moment coefficients are defined as non-linear functions of the angle of attack. These functions depend on a number of parameters, which may vary with the aerofoil, the Mach number and the Reynolds number. The various physical phenomena related to flow viscosity and separation are described separately. The viscous effects currently incorporated are the leading edge pressure lag, the boundary layer lag, the motion of the trailing edge separation point, the leading edge vortex separation, the reattachment process and (secondary) vortex shedding. The effect of a varying free-stream velocity is taken into account by making a correction on the downward velocity at the three-quarter chord, as proposed by van der Wall and Leishman [2].

ONERA has developed two dynamic stall models:

(1) ONERA-Edlin [6] is a general model based on the idea that the airloads can be described by well chosen linear second order differential equations, a set each for lift, drag and pitching moment. The differential equations are chosen to reproduce the small vibration amplitude behaviour of an aerofoil for each incidence and Mach number in the linear regime as well as in the stalled domain. This has normally led to a formulation where these two domains are distinct. The model thus defined works well in each domain on either side of the static stall angle. However, for large amplitudes of aerofoil oscillations, this boundary is modified requiring additional empirical modelling through classic time delays.
The model is able to simulate coupled pitching, plunging and in-plane motions, and has been extended to very large angles of attack (greater than 45°).

(2) ONERA-BH [8] is a recent model based on a Hopf bifurcation which aims at a better description of the vortex-shedding phenomena. Stall onset has been identified by replacing the time invariant equilibrium state of the flow field by a time-varying periodic equilibrium state as the angle of attack exceeds a critical value. The static values of the aerodynamic coefficients are governed by analytical relations adapted from the Leishman-Beddoes model [7]. This formulation accounts in a straightforward manner for various aerodynamic effects including sweep, blade rotation, 3D blade tip effects and Reynolds number effects.

WHL uses the dynamic stall models developed by Beddoes [7]. The method uses two time delays, one for the lift coefficient and the other for the pitching moment. Wagner functions are used for attached flow. The dynamic stall model applies for angles of attack in the range ±30° and in a limited region

around 180°, and a prescribed quasi-static representation of the aerofoil characteristics is used otherwise. Yaw effects are accounted by applying simple sweep rules.

Rotational effects

DLR and ECD do not use rotational effect models but for the DLR they could be represented in an manner analogous to that of yaw angles if considered to be significant.

DERA The effect of rotation on the lift coefficient beyond the onset of stall was not originally modelled in the initial calculations made with the rotor load code (CRFA). However the importance of the effect became apparent as the present work progressed, particularly for the very highly stalled cases. A correction, based on the ONERA model, was included in the analysis as an option and has been used for all the calculations used in this paper.

EC From the general 3D boundary layer equations it can be shown that, in the presence of centrifugal forces, the initially 2D boundary layer becomes 3D as soon as separation occurs. A radial flow appears accelerating the boundary layer and thus balancing the adverse pressure gradient. In this way rotational effects on a rotor delay stall and increase lift at the expense of increased friction drag in the pre-stall regime. This behaviour has been empirically modelled by directly correcting the basic 2D polar curves [9].
Parameters have been adjusted through rotor wind-tunnel experiments over the entire range of lift and advance ratios and a "universal" set of parameters has been fixed once and for all to match different rotor geometries.

NLR The effect of rotation on an aerofoil is taken into account by a simple empirical model based on the analysis of a wind turbine. The model adds some lift in the stalled domain. The amount of this added lift depends on the ratio of local chord to radius (c/r) and is highest at the blade root. Without rotation effects the 3D lift coefficient equals the 2D value. With full rotation effects the 3D lift coefficient is larger and approaches the 2D inviscid lift coefficient as boundary layer material is swept outwards. The model does not make any corrections to the drag and moment coefficients.

ONERA The effect of rotation on an aerofoil is taken into account by a simple model based on the work of Snel et al. [10]. This model simply states that rotation does not change the onset of stall but adds some lift in the stalled domain. The amount of lift that is added depends on the value of the chord to radius ratio. It is higher at the blade root and for deeper stall. This is a geometrical correction which does not depend on the rate of rotation.
The same form of correction is also used for pitching moment and drag, but the rotation effects are found to be negligible.

Comprehensive rotor codes

The DLR rotor code [1] is developed to simulate the dynamics of hinged or hingeless elastic blades by using their modal properties and their aerodynamics through the use of the 2D unsteady model in a wind tunnel environment (fixed shaft). Its purpose is also to provide high resolution lift distributions for noise calculations. The basis of the code is the blade element/lifting line theory, with a typical discretisation of 20 radial elements and 2° azimuthal steps. The 4-step Runge-Kutta integration gives an internal step size of 1°. The code is used for investigations of rotor performance, dynamic loads, active control and noise emission.

Essentially, four modules are connected by the main program. These are the blade equations of motion, the aerodynamics, the induced velocities, and the trim routine. All of these have a variety of options on blade motion, aerodynamics, wakes and trim conditions.

DERA The rotor load code used for the calculations is the coupled Rotor-Fuselage Analysis (CRFA) which is being developed jointly by the DERA and WHL. CRFA is a comprehensive, third generation analysis which can model an isolated rotor or a complete rotorcraft in steady or manoeuvring flight. Advanced features included in the method are the ability to model the flexibility of the transmission system via an impedance with a yaw degree of freedom and the representation of hub motion using an impedance with six degrees of freedom. The blade elasticity is represented by modes which are complex, i.e. have real and imaginary components, when hub motion is included. The method is extremely versatile and includes several options for modelling the rotor wake, the flow field about the fuselage and the integration technique in the radial and azimuthal directions.

ECD uses the CAMRAD/JA code. The structural model of the rotor is based on engineering beam theory (Bernoulli-Euler theory of bending). A modal representation based on the orthogonal modes of free vibration for the rotating blade is used to transform the partial differential equations describing the rotor blade motion to ordinary differential equations in time for the degrees of freedom. Separate modes are applied for the bending and torsion motion of the blade. The flap and lag bending modes are coupled in order to consider the in-plane and out-of-plane coupling of structural and inertial forces.
The rotor blade aerodynamic loading is calculated using lifting line theory and steady 2D aerofoil characteristics with corrections for unsteady and 3D flow effects. For low angles of attack thin aerofoil theory results are used to approximate the unsteady aerodynamic loading whereas for high angles of attack a dynamic stall model is used. The section aerodynamic characteristics are also corrected for the effects of yawed flow.
Trailed and shed vortices are considered in the wake model as vortex sheet panels or vortex line segments. The tip vortex is implemented with a definite vortex core limiting the maximum induced velocity. The rotor wake induced velocity is calculated by integrating the Biot-Savart law over all vortex elements in the rotor wake.

EC uses the last version of its R85 code [11,12]. This code calculates blade in-plane and out-of-plane bending as well as blade torsion, while taking into account elastic and aerodynamic centre offsets. The aerodynamics are represented by a lifting line model with a prescribed wake (METAR) using 2D aerofoil polar data. The elastic model is a fully non-linear beam and can account for large deflections as well as torsion/flexion and, to some degree, extension coupling.
The code solves the Lagrange equations to find a periodic solution projected on a given number of blade modes previously computed in rotation from the structural description of the blade. Usually 8 to 9 modes are necessary to provide good convergence on a realistic rotor.

The NLR rotor code is based on blade element theory in which the local flow at each blade element is assumed to be two-dimensional. The code calculates the rotor forces and moments by integrating the local blade element lift and drag forces along the radius and azimuth. For the rotor dynamics only the flapwise motion is considered. The first flapwise bending mode shape, which is dominated by rigid flapping, is obtained by iteration. For the induced velocity calculation

several models have been implemented, amongst which a prescribed wake model based on the METAR code of EC. The lift, drag and moment of the blade element sections, for given angles of attack and Mach numbers, are obtained by a table look-up method. These tables contain 2D steady aerofoil data.

To take unsteady effects into account, the dynamic stall model of Leishman and Beddoes [7] has been implemented.

Other specific 3D effects that are included in the program are corrections for tip losses, for yawed flow (correction on *Cz* and *Cd*), for cross-flow and for rotational effects.

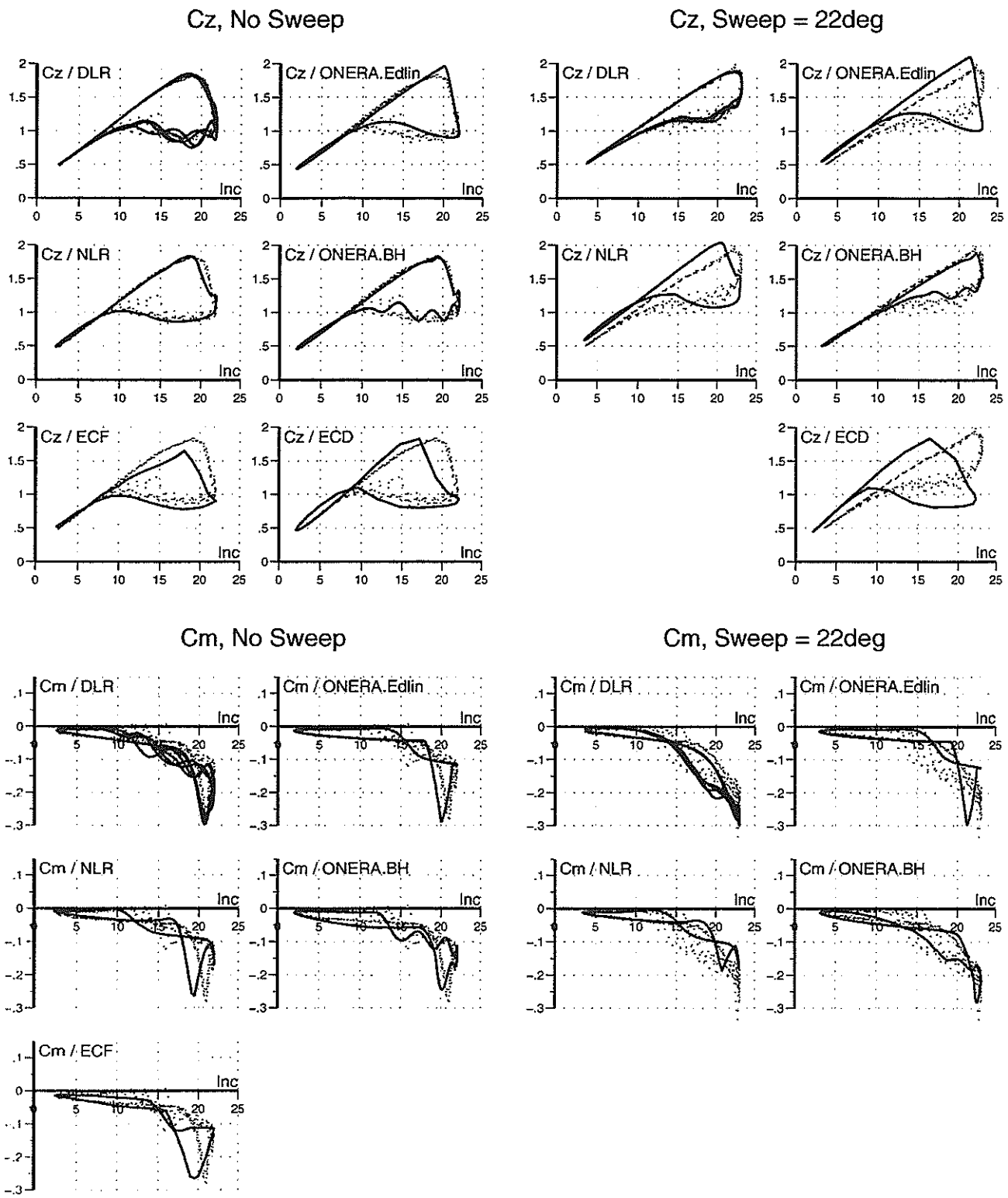

Figure 1. Cz and Cm hysteresis loops for normal and 22° swept flow on the OA213 aerofoil. Mach = 0.18, reduced frequ. = 0.05. Comparison between measurement (dots) and models

The ONERA comprehensive code [13] is based on the description of a rotor by a string of transformations that joins the general Galilean frame to the blade roots. These transformations consist only of pure translations or rotations and can be considered to be degrees of freedom or not. A particular transformation splits the string into *n* strings in order to simulate the *n* blades. The connected blades can have a 3D shape and are mechanically defined by a set of cantilevered modes.
This description of the rotor enables the study of a great variety of geometries: hinged or hingeless rotors, tethered rotors, propellers, wind turbines, etc. General airframes can also be taken into account by projecting the equations on a fuselage modal basis.
A set of routines computes the contribution of a blade element to the global equations of the aircraft. These equations can be used in a classic or a Floquet analysis to calculate forced periodic response, in time integration or for calculating structural modes.

Dynamic stall predictions versus experimental data

The dynamic stall models used by the different partners were first tuned in order to reproduce as well as possible the 2D large amplitude unsteady behaviour of the OA213 aerofoil. This was done for both normal flow and 22° sweep.

It should be noted here that for the case with sweep, the DLR and ONERA-BH models were directly tuned to the hysteresis loops obtained for that experiment while the other models were tuned only to the normal flow loops and the sweep effect were obtained through classic sweep corrections in the respective models.

The dynamic loops used were obtained with sinusoidal oscillations of 12° ± 10° of the angle of attack at reduced frequencies of 0.015, 0.05, and 0.10.

Typical results are shown in Figure 1.

Each partner's comments on the results

DLR The DLR aerodynamics allow an adjustment of the sweep effect, a point which coupled with the unsteady model perfectly matches the experimental loops, even in their fine details. The effect of frequency is perfectly taken into account. The experimental *Cz* oscillations in the stalled domain are reproduced thanks to the post-stall vortex shedding model. Their frequency is based on the Strouhal number and their phase (and to a lesser extent their amplitude) is random from on cycle to another.

ECD results are based on the steady curves from the steady data only. This induces the difference observed on the onset of stall. Taking this point into account, the figure shows that:
- *Cz* loops: The dynamic behaviour seems good with perhaps insufficient damping at reattachment.
- *Cz* loops with sweep: CAMRAD/JA refers to static lift, drag and moment tables without sweep. Sweep effects are introduced by using conventional aerodynamic corrections (effective angle of attack and dynamic pressure) which are obviously not appropriate for the present wind tunnel experiments.

EC uses the same steady curves as ECD. The result is that:
- *Cz* loops follow the measurements closely but stall is a little early.
- *Cm* loops also stall too early, but nevertheless reproduce the very negative experimental values.

NLR
- *Cz* loops: the calculated loops have the expected properties though the stall delay is slightly too small.
- *Cz* loops with sweep: the predicted stall takes place too early because the model has to follow the low (unstalled) values of the *Cz* data corrected for sweep. The lift is therefore too high, both during stall and during reattachment.
- *Cm* loops: the model predicts the large negative *Cm* values encountered at the onset of stall. The oscillations in the stalled domain are predicted by a vortex shedding model analogous to that of DLR.
- *Cm* loops with sweep suffer of the same problem as the *Cz* loops.

The ONERA-Edlin model was developed for easy application to all kind of aerofoils by simply starting from the static curves. Therefore, the steady coefficient differences from the two sets of data poses problems. The following behaviour is observed:
- *Cz* loops: the model prediction is good.
- *Cz* loops with sweep: loops are far too open because the model has to follow the classically sweep corrected steady *Cz* data.
- *Cm* loops: a new extension to the model reproduce the main features of the loops correctly.
- *Cm* loops with sweep: the model would reproduced the experimental loops much better if the real steady curves were used instead of the classic sweep correction.

The ONERA-BH model uses non-linear differential equations in order to deal with the sharp stall behaviour. Its main effect leads naturally to the oscillating airloads observed in the stalled domain and to an adjustable sweep correction. These features lead to generally satisfactory loops, both with and without sweep.

Conclusions

It should first be emphasised that the carefully measured steady curves in one experiment, and dynamic loops in another are to a certain extent inconsistent.
It is clear that the classic sweep effect correction used in most models does not measure up to the experimental data. This point will need further attention in the future.
Generally, when the difficulties due to the steady curves are disregarded, the dynamic models do quite well in reproducing loops which account well for stall delay, for frequency effects and, in some models, also for the vortex shedding phenomenon in post-stall.

Rotor code predictions versus experimental data

Introduction

The results obtained by the different partners lead to significant differences that need to be analysed. Unfortunately, dynamics and aerodynamics interact strongly when achieving the rotor equilibrium. It is difficult to assess whether discrepancies come from the dynamic or aerodynamic modelling. Mechanical approximations make the dynamic stall models work in the wrong angle of attack domain and give biased results, and conversely, aerodynamic modelling changes the rotor equilibrium.

Trimming to thrust usually helps putting the rotor into the right working conditions when controls and induced velocities are not well defined. But for very high levels of thrust, trimming to the rotor thrust creates problems for models which have difficulties in reaching the high experimental loads. As the curve of

load versus collective pitch becomes quite flat at high loads, these models reach equilibrium at collective pitch angles that are far too large. In fact, trimming to thrust as against prescribed control angles mainly measures the way high loads are taken into account in the models through lift corrections due to yaw or rotation effects.

For the sake of conciseness, only results obtained with prescribed control angle are presented in this paper. These give the clearest comparative picture of the code capabilities. Lift and moment on the blade are shown at two spanwise sections in Figures 2 and 3 for the standard chosen test case. Blade root torsional moment and blade tip torsion are shown in fig 4 for two test cases because the standard case (highest thrust) data do not include blade tip torsion, the lower thrust case therefore allows comparison with experiment.

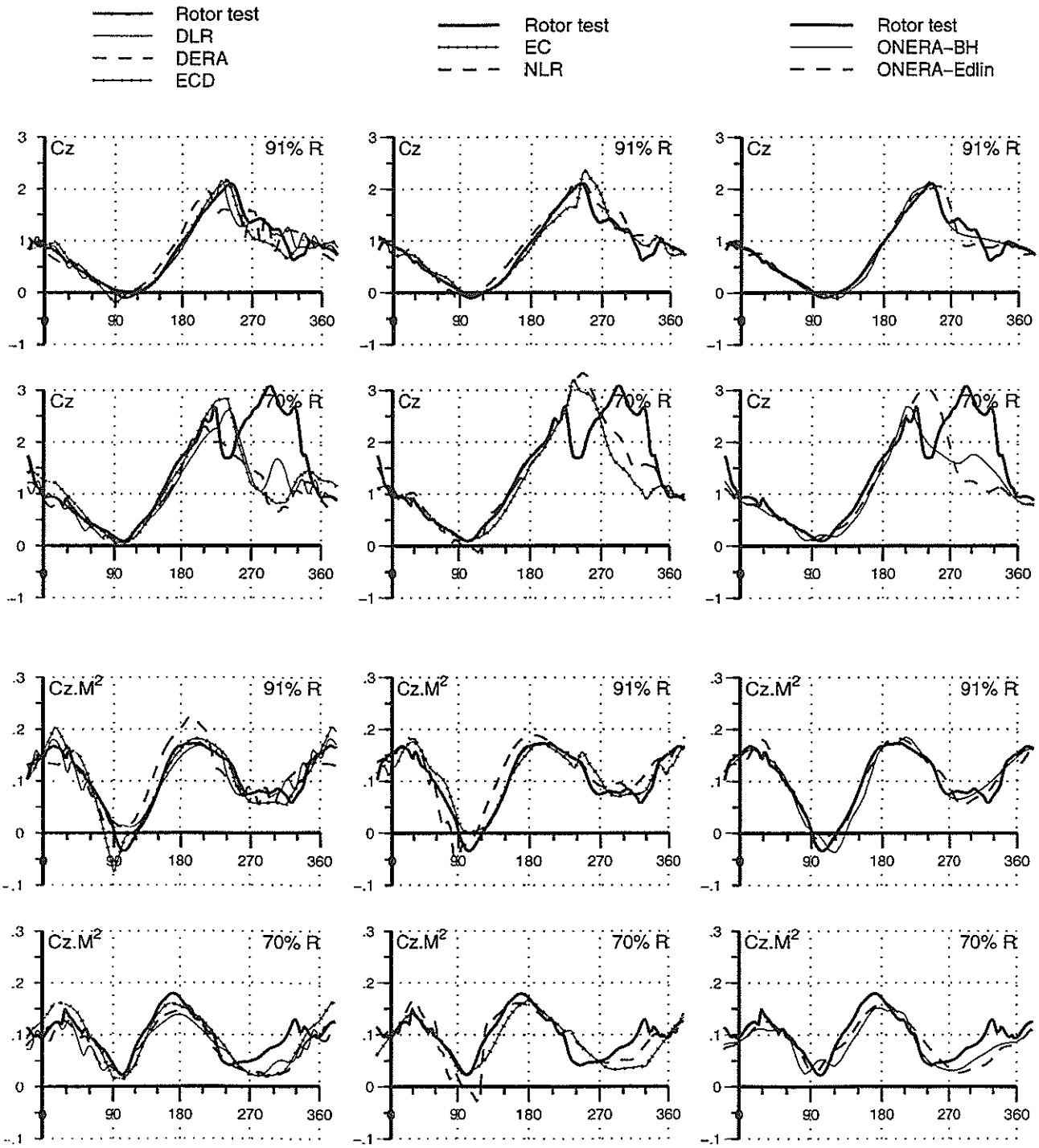

Figure 2. Lift coefficient, Cz, and lift force, CzM², as a function of azimuth for $C_T/\sigma = 0.125$. Measurements versus models at 70% and 91% radial positions

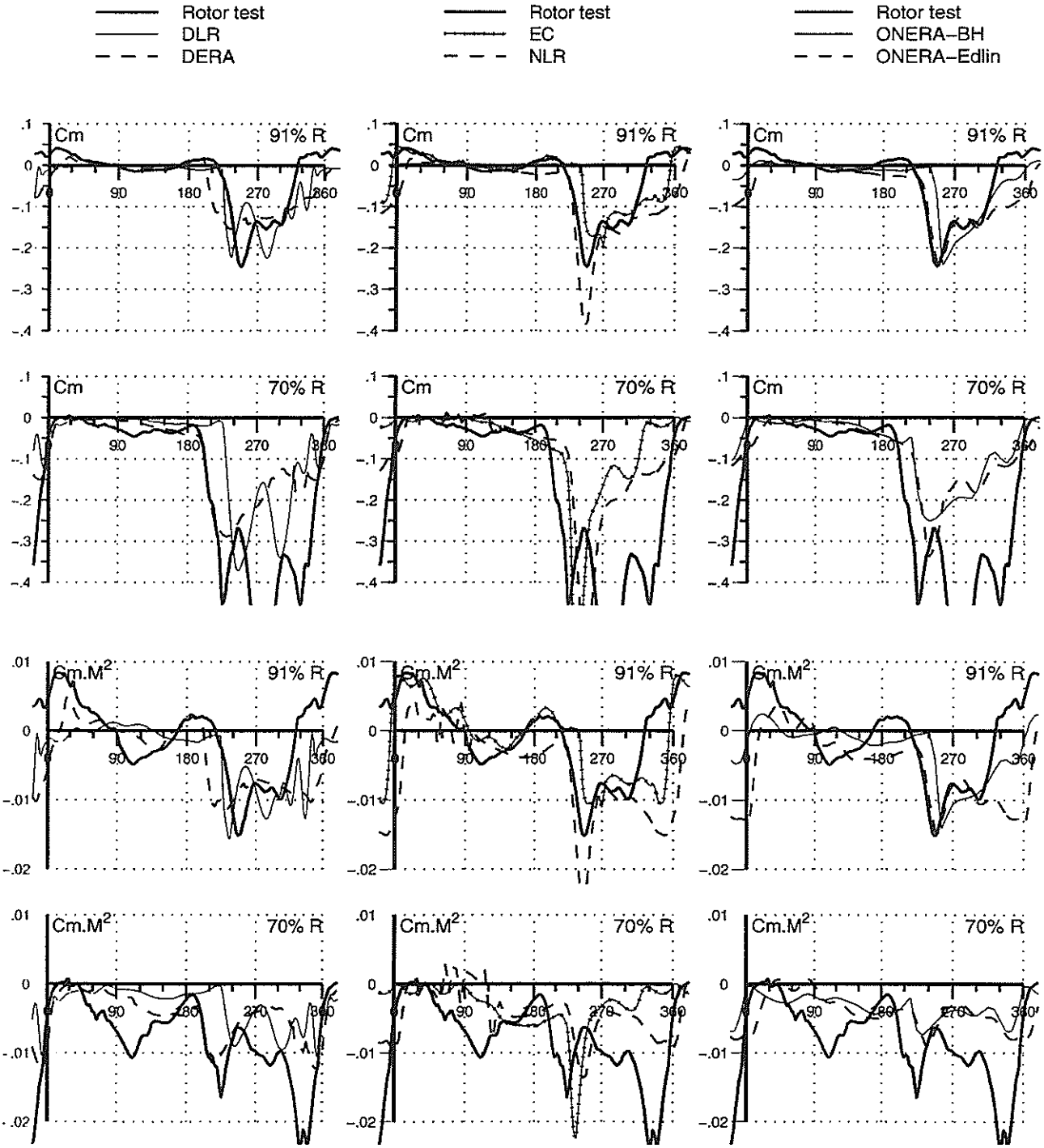

Figure 3. Moment coefficient, Cm, and pitching moment, CmM², as a function of azimuth for $C_T/\sigma = 0.125$. Measurements versus models at 70% and 91% radial positions

Each partner's comments on the results

DLR From the set of parameter variations investigated, it is apparent that from an aerodynamic point of view the following four major effects must be taken into account:

1. Unsteady aerodynamics in order to obtain the time lag behaviour and to alleviate the spikes due to large angle-of-attack variations when BVI is present.
2. Dynamic stall in order to obtain lift overshoot due to delayed stall onset.
3. Variable velocity effects in order to obtain the large incidences on the retreating side.
4. Yaw effects in order to delay stall by a significant amount. The sharp moment spike at stall onset is produced by the first stall vortex passing the trailing edge. A secondary vortex shedding needs to be included when the post-stall fluctuations in lift and moment are to be predicted.

DERA The calculated lift coefficient shows that the analysis predicts stall too early in azimuth at the outboard sections,

presumably because of the poor modelling of sweep effects, but the correlation improves further inboard. The quasi-steady aerodynamic representation under-predicts the lift coefficient and is particularly apparent at 70% radius in the third and fourth quadrant of the disk. The comparisons between the measured and calculated CzM^2 show the differences more clearly, especially the phase error at 91% radius.
The premature blade stall predicted by the analysis at the outboard stations is very apparent from the comparison with the measured pitching moment coefficient. The change in pitching moment at the break is underestimated also by the unsteady aerodynamic model. The poor prediction of the pitching moment coefficients is emphasised when compared with the measured CmM^2.
The predicted torsional displacement at the blade tip shows that stall onset occurs at about 200° azimuth and that there is a strong 8-9 per rev oscillation. The calculation shows the same high harmonic activity but the phasing is incorrect because the stall onset occurs too early in the azimuth cycle.

The ECD calculations based on the CAMRAD/JA code and stall modelling were partially successful. The predicted dynamic lift section coefficients show the characteristic dynamic overshoot. The operating conditions of the analysed case are based on significant non-linear phenomena occurring at stall. Consequently trim algorithms are very sensitive to small deviations.
The 2D loop results show some deficiencies concerning the sweep angle effect. Obviously the lift overshoot due to the sweep angle is underestimated in the current model. But this fact has no significant influence on the final results.

EC Lift at 91% of the blade is correctly predicted especially on the retreating side where stall occurs. However, one can notice a lack of negative Cz on the advancing side (at 100°) and a slightly different Cz slope in the second quadrant. Due to high Mach numbers in this region, the lift produced on the advancing side is over estimated. This might come from a small error in the level of torsion in this region: 0.5° of torsion would make the difference.
Pitching moment at 91% is correctly predicted by the code on the advancing side, with the help of the unsteady Theodorsen formulae. In the region of stall the code shows a 10° azimuth delay for stall onset compared to experiment and under-predicts dynamic stall effects. However, the leading edge vortex responsible for this sharp negative Cm has been correctly predicted but the under-prediction of Cz at the vortex formation and separation (200° and 220°) explains the lack of negative Cm since the latter is highly dependant of the accuracy of the former.
At 70% of the blade, the ECF model slightly over-predicts high Cz. Moreover, the model does not predict the second increment of lift in the aft part of the rotor, which might be due to successive vortex shedding during the deep stall process. Indeed, the model has not been developed to account for these secondary phenomena which have little effect on the pitch link loads.
The peak-to-peak level of the torsional moment at the blade root is correctly estimated guaranteeing good predictions of the pitch link loads. As in the experiment, the pitch link load peak is predicted to occur at 240° azimuth which is typical of stall onset on a rotor. The harmonic content is at the torsion frequency of the blade (8-9 per rev).

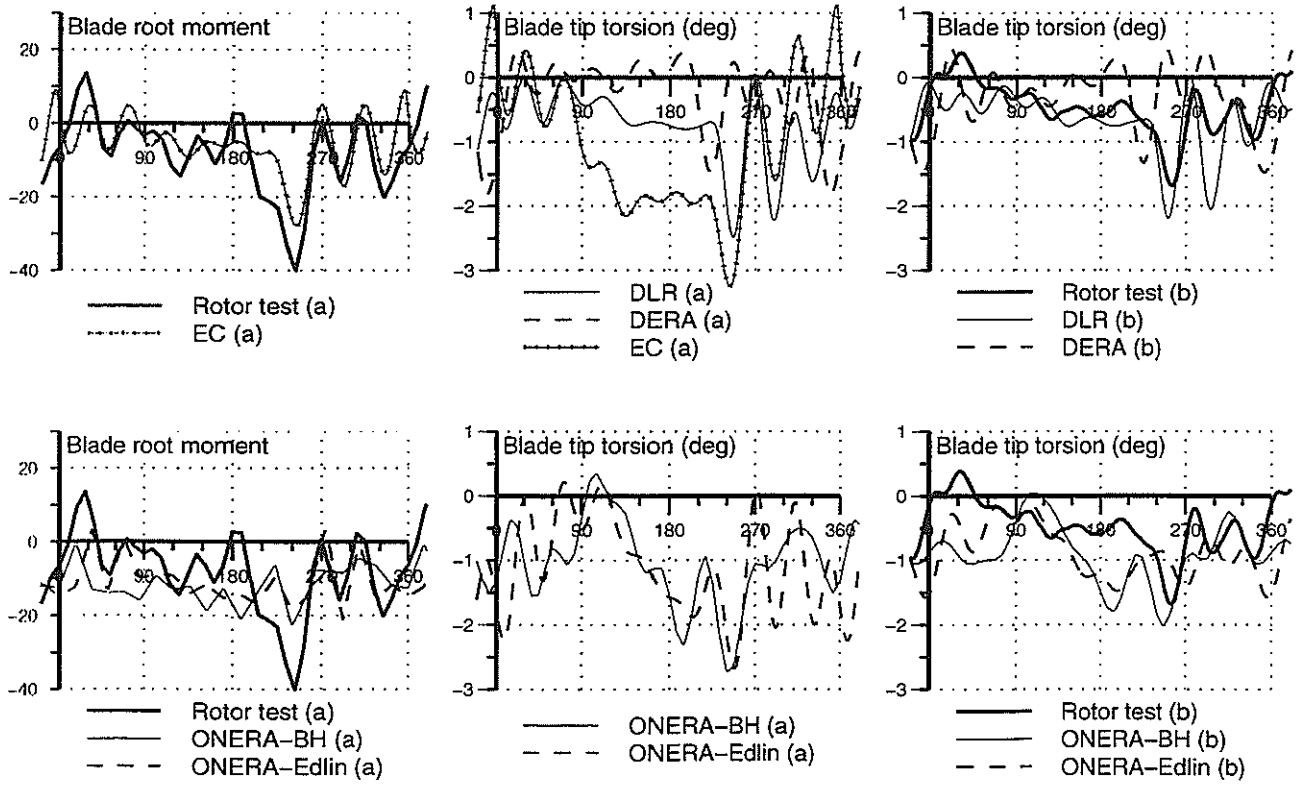

Figure 4. Torsional blade root moment and blade tip torsion as a function of azimuth. Measurements versus models.
a) standard test case ($C_T/\sigma = 0.125$) with no blade tip torsion measurements
b) test case with $C_T/\sigma = 0.112$ comparing blade tip torsion measurements and predictions

The NLR rotor code predicts the properties of *Cz* and *Cm* in most cases: the delayed onset of stall, the dynamic overshoot in lift, the large negative peaks in *Cm* (especially on the outer part of the blade), and the secondary vortex shedding which mainly manifests itself on the moment coefficient. The only problem is an azimuthal phase shift in the local lift of about 20° to 30° at the outer blade sections. The correction for rotational effects produces a considerably smaller increase in lift than the partners' models.
All NLR calculations have been made for torsionally stiff rotor blades, and therefore torsional deflections and pitch link loads are not available. However, the differences between the NLR's overall results and those of the partners with flexible blades are small.

The ONERA comprehensive rotor code together with the Edlin dynamic stall model generally gives satisfactory results. Lift is well predicted in amplitude and phase, as well as the large negative peak of moment at the onset of stall. Large lift and moment values at mid-blade are obtained, although not large enough for the moment. The empirical correction due to rotation considerably improves the results.
Nevertheless, two important points are missing in the model. The first is the secondary peak in lift and moment in the deep stalled region. The second is the absence of the positive *Cm* peak observed at azimuth 180° all along the blade span. This last point may be responsible for the excessive negative torsion calculated at this azimuth.
The rotor code with the BH dynamic stall model improves the unsteady moment at all spanwise sections leading to a better blade torsional moment. However, the model also gives rise to large undamped torsional oscillations which are not found in the experiment. This point needs further investigation.

Parameter effects on the comprehensive rotor codes

A better insight into the effect of the aerodynamic models and of blade flexibility is obtained by looking at the isolated effect of these parameters. Calculations were made for the standard test case with prescribed control angles and the following four separate computation configurations:

1. stiff blades, stall models and no aerodynamic corrections
2. stiff blades, stall model and aerodynamic corrections
3. stiff blades, quasi steady aerodynamics and aerodynamic corrections
4. soft blades and dynamic stall models with aerodynamic corrections

Some of the results are shown in the table below. A study of this table leads to the following conclusions on the effect of the models on rotor performance predictions:

Aerodynamic corrections. Comparing configurations 1 and 2 shows the effect of the two main aerodynamic corrections which are yaw and rotation effects. These are necessary in the models in order to trim to thrust.
All the models show a very significant effect of these corrections varying from 373N (NLR) to 742N (ONERA). A decomposition of the ONERA result into sweep and rotation corrections shows that rotation contributes about 35%.
These aerodynamic corrections generally lead to a decrease in the required shaft power, but the scatter here is very large. The gain in power is as much as 20% for ECD but DERA shows a loss of 6%.

Dynamic stall model (configs. 2 and 3). By replacing the dynamic stall model in configuration 2 by quasi steady aerodynamics in configuration 3 one can estimate the effect of the models for this very heavily loaded case.
The dynamic stall model adds an average of 3% to the thrust (from -2% for ECD to 8% for DLR). The effect on power is also relatively small: from a loss of 7% (NLR) to a gain of 3% (DLR).
One also notes a large effect of the models on the longitudinal blade flapping angle: of the order of 2°.

Blade flexibility (configs. 3 and 4). Adding flexibility to the blade has the effect of changing the local aerodynamic incidences due to a pitch down torsion of the blade (not for NLR's model which considers that the blades are rigid in torsion) as well as to elastic blade flapping. The models find a slight decrease in lift but agree in an approximate 8% decrease in the required shaft power (except for ECD).

Vertical force (*N*), experiment: 3646				
configuration:	1	2	3	4
DLR	2828	3455	3198	3406
DERA	3182	3530		3507
ECD	3465	4201	4270	4238
EC	2919	3640	3597	3556
NLR	3284	3657	3461	3640
ONERA	2939	3681	3632	3663
WHL		3704		3740
Shaft power (*kW*), experiment: 72				
configuration:	1	2	3	4
DLR	77	73	71	65
DERA	50	53		51
ECD	81	65	65	66
EC	80	78	80	73
NLR	70	65	70	65
ONERA	84	74	74	68
WHL		44		37

These indications can be useful for design offices to evaluate the necessary sophistication of their prediction codes. However, a more detailed study shows that the effects of the models are of course quite different on the unsteady load predictions.

Discussion of aerodynamic model predictions in the light of the rotor tests

Blade vortex interaction (BVI)

Blade vortex interaction can be seen at the rear part of the rotor, especially on the advancing side. ECD, EC and ONERA calculations seem to filter out these effects. On the other hand, the DLR and NLR calculations emphasise them when compared to experiment. This is particularly obvious on the CzM^2 results. The DERA's results are closest to experiment from the BVI point of view.

Aerodynamics in the non stalled domain

The linear unsteady lift does not depart significantly from the quasi-steady lift. The linear unsteady moment, on the other hand, is not negligible Theoretical effects create a small negative moment coefficient when the blade is fore.
However, the experimental results display a strong negative moment on the advancing blade, followed by a steady increase in moment that peaks just before stall. Although the models predict an increase in moment just before stall (particularly EC at the blade tip), the overall phenomenon is never reproduced. As this phenomenon is present all along the

blade span it cannot be attributed to 3D unsteady effects and remains unexplained. This effect is particularly strong on CmM^2 due to the high Mach number, and is thus important from the blade dynamics point of view.
The linear unsteady moment also has an influence on the torsional damping. It is clear from the torsion predictions that the aerodynamic torsion damping issued from the models is generally a little too small.

The onset of stall

The onset of stall is not a characteristic of the unsteady aerodynamic models. It comes from the working conditions of the aerofoil which are the result of the interaction between the dynamics and the aerodynamic lift through the rotor equilibrium. The prediction of the onset of stall on the pitching moment happens to be a fine measure of the overall quality of the model.
It should be noted that the rotor tests exhibit a later stall at the blade tip than at the blade root. This phenomenon is reproduced by the EC and ONERA models, although they both stall too late. On the other hand, the DLR and NLR models predict the onset of stall well at the blade tip but are a little late at the root. The DERA model is correct at the blade root but in advance at the tip.

Lift stall delay

The different models have included features that take stall delay into account in a very similar way. They match experiment at section 91% but in general lead to late stall at more inboard sections while still remaining acceptable.

Lift in deep stall

The peaked deep stall domain on the outer sections of the blade is well represented by the different models.
As one moves inboard from the blade tip a secondary peak of *Cz* progressively appears in the stalled domain. This merges with the first peak at mid-blade to create a wide zone of very large *Cz*. This secondary peak (fig. 2) is present in the DLR results, though not as large as in the experimental data, and it can be distinguished in the NLR calculations. The ONERA-BH model gives high *Cz* values in the stalled domain which can be attributed to rotation effect corrections.
It seems that the secondary *Cz* peak is due to a vortex shedding mechanism (DERA, NLR) which may be considerably enhanced by rotation effects (ONERA-BH). It is fair to add here that the influence of this phenomenon on CzM^2, and thus on the rotor behaviour, remains small due to low Mach numbers.

Moment in deep stall

Generally, moment behaves in the same way as lift. Starting at the tip section of the blade, measurements first show a strong negative peak of moment occurring at the onset of stall. Although DERA gets large negative *Cm* values, the observed peak is absent. On the other hand, EC's negative peak is too narrow and deep but seems globally to produce the impulsive force needed to predict blade torsion correctly.
When one moves inboard, moment still becomes negative abruptly, but there is no longer an isolated peak and the whole stalled region reaches very negative values. As for the lift, a kind of a secondary peak is present here and the same conclusions seem to apply. This peak is detected by DLR and NLR predictions.
Cm acts on the blade according to the value of CmM^2. Negative blade root moment is found by the EC model. This is because the azimuth at which stall is found with these models is early enough for the Mach number to have kept the high value needed to create the large observed impulse on the blade.

Blade torsional moment

Blade torsional moments are not given by all the partners. The experimental blade moment behaves much as expected following the measured local *Cm*. The main features are:
— A positive peak at 180° azimuth which the calculations ignore.
— A negative peak at 240° azimuth due to stall. This is reproduced by the EC and ONERA calculations at the blade tip and by EC only at the blade root.
— Oscillations following the onset of stall which are damped out at 60° azimuth.

Blade torsion

Blade torsion was unfortunately not measured for the highest load case reported here in all the results. For this reason a less loaded test case is also shown in figure 4. It seems as if the rotor behaves in the same way for the two cases except for lower intensity levels for the smaller loading.
At 180° azimuth the *Cm* of the ONERA and EC codes gives a negative torsion of 1.5° to 2° whilst the DLR and ECD results follow the experiment more closely with 1°. This torsion is due to the high lift on the blade's parabolic tip which should be balanced by the positive aerodynamic moment ignored by the calculations. The DERA model seems to work here as if the blade were rectangular.
The excitation due to stall is reasonably predicted by all the models that give high negative *Cm* values. This is followed by oscillations that generally damp out more rapidly in the experiment than in the predictions.

Conclusions

It must be emphasised that the unsteady 2D aerofoil models used in this benchmark were identified on a simple test performed at one Mach number on one aerofoil. Moreover, this test showed that the classic yaw corrections do not apply very well here. Nevertheless, predictions of rotor loads for a difficult flight condition are reasonably accurate. Taking into account all the aerodynamic corrections, the codes usually predict stall roughly at the right moment with fairly good maximum values of *Cz* and *Cm*.
Due to the large influence of the Mach number factor, the azimuthal location of the onset of stall is an important parameter for predicting the vibration levels of blades. The successful prediction of this location depends on very good modelling of all the rotor parameters.

A significant feature shown by the rotor data is the presence of a large secondary peak of aerodynamic forces that appears some time after stall over a large area of the blade. Several models suggest that this is due to a vortex shedding mechanism which may be enhanced by rotation effects.

The pitching moment has strong negative values all along the span of the advancing blade followed by a steady increase during a quarter turn of the rotor. No model is able to reproduce this phenomenon. More research is required here.

This common exercise between several European research centres and manufacturers has considerably improved the understanding of unsteady rotor aerodynamics and has enabled all the partners to improve their prediction capability.

References

1. van der Wall, B.G., "Analytic Formulation of Unsteady Profile Aerodynamics and its Application to Simulation of Rotors", ESA-Report No. ESA-TT-1244, 1992.

2. van der Wall, B.G. and Leishman, J.G., "The influence of variable flow velocity on unsteady airfoil behaviour", in "18th European Rotorcraft Forum", Avignon, September 1992.

3. Johnson, Wayne, "CAMRAD/JA. A Comprehensive Analytical Model of Rotorcraft Aerodynamics and Dynamics Volume I: Theory Manual".

4. Gormont, Ronald E., "A Mathematical Model of Unsteady Aerodynamics and Radial Flow for Application to Helicopter Rotors", USAAVLABS TR 72-67, May 1973.

5. Johnson, Wayne, "The Response and Airloading of Helicopter Rotor Blades due to Dynamic Stall", Massachusetts Institute of Technology, ASRL TR 130-1, May 1970.

6. Petot, D., "Modélisation du décrochage dynamique par équations différentielles", La Recherche Aerospatiale #5, 1989.

7. Leishman, J.G. and Beddoes, T.S., "A generalised model for airfoil unsteady aerodynamic behaviour and dynamic stall using the indicial method", in "42nd Annual Forum of the American Helicopter Society", Washington D.C., June 1986.

8. Truong, V.K., "Prediction of helicopter rotor airloads based on physical modelling of 3-D unsteady aerodynamics", in "22nd European Rotorcraft Forum", Brighton, September 96.

9. G Arnaud, G., Benoit, B., Toulmay, F., "Amélioration du modèle d'aérodynamique du code rotor hélicoptère R85", in "28eme colloque d'aerodynamique appliquée", ISL, France, Octobre 91.

10. Snel, H., Houwink, R., Piers, W.J., "Sectional prediction of 3D effects for separated flow on rotating blades", in "18th European Rotorcraft Forum", Avignon, France, September 92.

11. Benoit, B., Arnaud, G., "Simultaneous treatment of torsion and flexion in the aeroelastic R85 code", in "18th European Rotorcraft Forum", Avignon, France, Septembre 92.

12. Toulmay, F., Arnaud, G., Falchero, D., Villat, V., "Analytical prediction of the rotor dynamics for advanced geometry blades", in "52nd American Helicopter Society Forum", Washington, June 96.

13. Petot, D., Bessone, J., "Numerical calculation of helicopter equations and comparison with experiment", in "18th European Rotorcraft Forum", Avignon, France, September 92.